

RSC Advances



This is an *Accepted Manuscript*, which has been through the Royal Society of Chemistry peer review process and has been accepted for publication.

Accepted Manuscripts are published online shortly after acceptance, before technical editing, formatting and proof reading. Using this free service, authors can make their results available to the community, in citable form, before we publish the edited article. This *Accepted Manuscript* will be replaced by the edited, formatted and paginated article as soon as this is available.

You can find more information about *Accepted Manuscripts* in the [Information for Authors](#).

Please note that technical editing may introduce minor changes to the text and/or graphics, which may alter content. The journal's standard [Terms & Conditions](#) and the [Ethical guidelines](#) still apply. In no event shall the Royal Society of Chemistry be held responsible for any errors or omissions in this *Accepted Manuscript* or any consequences arising from the use of any information it contains.

ARTICLE

Synthesis, in-silico screening and preclinical evaluation studies of hexapeptide analogue for its antimicrobial efficacyCite this:
10.1039/x0xx00000x

DOI:

Ankur Kaul, Anjani K. Tiwari, Raunak Varshney, and Anil K. Mishra

Received 00th January 2012,
Accepted 00th January 2012

DOI: 10.1039/x0xx00000x

www.rsc.org/

A novel Trp-Arg rich antimicrobial peptide was designed and the synthesized nonapeptide (hexapeptide analogue AMP) was screened for its antimicrobial activity and hemolytic activity. The *in-silico* studies were performed further against the microbial targeted protein to validate the findings. *In vivo* studies were carried out for preclinical evaluation of the designed peptide sequence was carried out using ^{99m}Tc as radioisotope. The results obtained from the *in vitro* studies revealed that the excellent antibacterial activity against *E.coli* with low hemolytic activity. The in-silico studies with the crystal structure of *E.coli* Penicillin Binding Protein 1b (PBP1b) glycosyltransferase (PDB ID: 3VMA) shown higher electrostatic and hydrophobic interactions than the co-crystallized ligand. The radio labeling yield of the ^{99m}Tc -labeled AMP was found to be > 98% and the blood-kinetics in rabbits and the biodistribution studies in mice confirmed the rapid renal excretion from the systemic circulation. The scintigraphic analysis in infection and inflammation animal models revealed that the radiolabel was able to discriminate between the infection and inflammation in both mice and rats. Furthermore, the blocking experiments in scintigraphy were also done using cold peptide to confirm the specificity towards the *E.coli* infection. Based on above findings, we consider the designed AMP as a novel antimicrobial agent with ability to image bacterial infection *in vivo* by application of gamma emitting radioisotope.

Introduction

As the crisis of looming menace of bacterial resistance to currently available antibiotic persists to grow, a substantial significance is being given to explore the option of development of antimicrobial peptides as a novel therapeutic approach as an antimicrobial chemotherapy.¹⁻³ Antimicrobial peptides have the unique characteristic of the natural defence mechanism which occurs practically in all the forms of life organisms ranging from unicellular to multi-cellular organisms^{4,6}. The mechanism of anti-bacterial action of the antimicrobial peptides is possibly by interacting with bacterial membrane proteins which is critical to their antimicrobial property, but their ultimate site of action is usually intracellular.⁷⁻⁹ Since our armory of anti-infective is getting older and less efficacious, the R & D activities are being diverted to identify templates of novel antimicrobial peptides by using newer methods of Computer Aided Drug Design (CADD) such as docking to decipher how antimicrobial peptides would interact with membranes *in-vivo*.¹⁰⁻¹² The combinatorial chemistry approach is regarded to be an additional option that is competent of screening and assorted collection of different peptides in a short time and recognizing those that have the novel or enhanced properties. Many of these peptides have been screened and isolated from nature and the synthetic combinatorial library.¹³⁻¹⁵

Our group has been working in infection imaging field in the past¹⁶ and here, report the design, synthesis and docking studies and its

antimicrobial activity for application in systemic diseases. The study was planned to include *in-silico*, *in-vitro* and *in-vivo* studies for the assessment of the antimicrobial efficacy of the designed ligand. The aim of current study to develop an infection imaging agent which would interact with targeted membrane protein to a greater extent and the selection of correct ligand for in vivo infection visualization would be done through CADD platform. The visual image of the target-site would be traced by a radioisotope tagged to the antimicrobial peptide as a signal emitter. In the past, many radiolabeled antimicrobial peptides have been evaluated for the infection imaging application.¹⁷⁻²⁰ In this study, first, an antimicrobial peptide sequence was designed, based on 'templates derived from naturally occurring antimicrobial peptides' and making the amino-acid sequence viable for radiotracer conjugation for signal detection. To start with *in-silico* screening studies, these were carried out for the newly designed peptide with the available microbial target to understand its extent of interaction with target proteins. Then, the *in-vitro* study involved evaluation of antimicrobial activity against commonly occurring bacterial strains. For *in-vivo* studies, the post radiolabeling, various studies like Blood-clearance studies, Tissue-distribution studies and further Gamma scintigraphy in animal model of infection and histopathological studies were carried out to examine whether this hexapeptide template linked to tripeptide (Gly-Gly-Cys) chain when labeled with a radiotracer would facilitate the imaging of infection non-invasively.

2.0 Materials and Methods

2.1 Materials

Wang Resin and Fmoc-amino acids such as Gly, Phe, Arg (Pbf) Trp(boc)- diisopropylcarbodiimide (DIC), triisopropyl silane (TIS), 1,2-ethanedithiol, piperidine solution (20% (v/v) in DMF) were procured from Fluka (USA). N, N-diisopropyl ethylamine (DIPEA), Trifluoroacetic acid (TFA) were purchased from Merck Germany. N, N-dimethylformamide (DMF), and stannous chloride were purchased from Sigma-Aldrich Co. (USA). HOBt was obtained from Hi-Media, India and tissue culture media were obtained Fischer Scientific (USA).

2.2 Instrumentation

The docking studies were carried out using Glide® (Schrodinger, USA). Mass spectroscopy (ES+MS) experiment was recorded on an Agilent 6310 Ion trap LCMS while Freeze drying was done using Triad System from Labconco, USA. Capintech, Caprac-R gamma scintillation well-type counter was used for the determination of activity. The reverse HPLC 1200 series with C-18 column Zorbax ODS 5 micron from Agilent Technologies was utilized for HPLC analysis

2.3 Experimental Animals

All animal experiments protocols were approved by the INMAS Animal Ethics Committee guidelines. BALB/c strain mice of 20–25 g and Sprague dawley rats of 220-250g were used for biodistribution and scintigraphic studies. New Zealand albino rabbits of 2-3 kg were used for the blood clearance studies. *E. coli* bacilli for the development of the animal model of infection.

3.0 Experimentation Section

3.1 In-silico studies

3.1.1 Computational Methodology

A molecular modeling study was performed by using schrodinger molecular docking program GLIDE²¹, version 9.7. During the process of Docking, Glide carries out a systematic search of best possible conformers of docked ligand with target protein with energy optimisation method. PDB entry 3VMA, (X-ray crystal structure of Penicillin-binding protein 1B; www.rcsb.org), having the resolution of 1.6Å were taken for our studies. The following criteria were keeping in mind before choosing the protein- ligand complexes: non-covalent binding between protein and ligand, crystallographic resolution less than 2.5 Å and known experimental binding data. Preparation of the protein for docking included removal of unnecessary heteroatom and solvent coupled with the addition of hydrogen atoms, bond order for crystal ligand and protein were adjusted and minimized up to 0.30 Å RMSD. Using 'Glide grid generation' the binding region was defined by a 17.04_9.31_0.58 Å box centred on the centroid of the crystallographic ligand to confine the centroid of the docked ligand. No scaling factors were applied to the Van der Waals radii. Default settings were used for all the remaining parameters. Scores in form of GScore were analysed for two purposes: during the docking process, they serve as fitness functions in the optimization of ligand orientation and conformation, and for comparison with other molecules they are used as estimates of binding affinity for the completely docked molecule.²²

3.2 Peptide Synthesis

The hexapeptide analog template was synthesized using the Standard solid phase synthesis technique on Wang resin support using the Fmoc-chemistry.²³ The first amino acid was anchored onto the wang resin by adding a mixture consisting of excess Fmoc-Gly-OH and HOBt and DIC in DMF. All other amino acids were coupled by dissolving an excess (4 mol equiv.) of Fmoc-protected amino acid, HOBt, and DIC in DMF. Removal of the N-terminal Fmoc group was performed using a 20% (v/v) solution of piperidine in DMF for 20 min. Amino acid side chains were protected using protecting groups like BOC (Trp) and PBF(Arg).The nonapeptide RRWWRFGGC-NH₂ was synthesized with high yield. The peptide was acetylated by using acetic anhydride in the solvent and the Acetylated Peptide with an overall yield of 95% after HPLC purification. Peptide was characterized by the retention time during elution of the pure form by analytical RP-HPLC and was also characterized by mass spectroscopy.

3.3 In-Vitro Studies

3.3.1 Antimicrobial activity assessment studies

The antimicrobial activity of the synthesized peptide was tested against six bacterial strains by the microdilution technique. The aliquots of 100µl of specific bacterial suspension (2×10^6 colony forming units) (CFU) ml in 1% peptone were added serial dilutions of 100µl peptide solution. After incubation of 18-20 h at 37°C, MIC values in µM were determined by measuring absorbance at 620 nm with the microplate reader.

3.3.2 Hemolytic activity studies

The assessment of the hemolytic activity of hexapeptide analog was done using erythrocytes from the heparinized human blood sample. Red blood cells extracted, were diluted to 1% and incubated with various dilutions of peptide stock (ranging from 1 to 1000 µg/ml) at 37°C for 60 min. After centrifugation at 4000 rpm for 5 min and the supernatant of incubated samples were collected for spectroscopic analysis at 540 nm. 100% Hemolysis was defined by lysis by 1% Triton X-100. The experiment was set in triplicate, and Hemolytic level was expressed by the % Hemolysis was estimated by the ratio of the value measured for each sample and that registered for the total hemolysis.

3.3.3 Radio labeling Studies

The various parameters like concentration of stannous chloride, pH of the solution, incubation time were optimized to obtain high Labeling Efficiency. The % Labeling Efficiency of the radiolabel was estimated chromatographically using ascending Instant Thin-Layer Chromatography using silica gel-coated sheets (ITLC-SG) strips (Pall Corporation, USA) as the stationary phase and methyl ethyl ketone (MEK) as a mobile phase and the radioactivity was determined using gamma counter.

4. *In-Vivo* Studies

4.1 Blood- clearance studies

Blood clearance study was carried out in normal albino New Zealand rabbits ($n = 03$) 0.2 ml of radiolabeled hexapeptide analog was administered intravenously through the dorsal auditory vein. At different time intervals starting from 5 min up to 24 h post i.v. administration and the blood samples were collected in pre-weighed tubes and counted for radioactivity using the gamma counter. Radioactivity in blood circulation after decay correction was expressed as percent of the total activity in the blood volume taken 7.3% of total body weight as the weight of whole blood.

4.2 Tissue distribution studies

Tissue-distribution studies were carried on BALB/c mice ($n = 03$) post i.v. administration of 0.1 ml of radiolabeled peptide through the tail vein. The animals were sacrificed at 1 h, 4 h and 24 h post injection and various organs of interest were removed and collected into pre-weighed tubes and their corresponding radioactivity was counted using the gamma counter.

Radioactivity accumulated in each organ was expressed as percent administered dose per gram of tissue (% ID per gm). It was calculated after decay correction.

4.3 Gamma Scintigraphic studies

The gamma scintigraphic study was designed to carry out two sets of experiments in normal rats and in *E.coli* infected animal models. For preparing animal models of infection and inflammation, BALB/c mice ($n = 03$) were infected in anterior right caudal muscle with the *E. coli* suspension (1×10^9 (CFU) Colony Forming Units/ 100 μ l and carragenan solution respectively. Twenty-four hours after the inoculation, BALB/c mice were imaged on Siemens Symbia $\text{\textcircled{R}}$ gamma camera 1 h and 4 h after i.v. administration of radiolabeled peptide. The pre-blocking experiment was also carried out by pre-injection of unlabeled peptide solution and then i.v. administration of radiolabeled peptide in the same infected rats.

4.4 Histopathological studies

The three random specimens of the *E.coli* infected muscle were dissected from the infection model developed in mice and were stored in the formalin solution. The specimen along with a control muscle sample (injected with normal saline) was sent for histological examination. The dyes like hematoxylin and eosin (HE) were used to stain the specimens and then viewed by microscopy and the photographs were taken for interpretation and validation of the infection model.

5.0 Results and Discussion

Peptide Antimicrobial agents form a component of the early innate and the first line of defence for the majority of living organisms.²⁴⁻²⁶ The distinct attribute of peptide-antibiotic is its selectivity.² When in competition with host and bacterial cells, the antimicrobial peptide will interact with the bacterial cell in preference to mammalian cells, which enables it to destroy microbes without being extensively toxic

to host cells.^{4,7} Hence, these antimicrobial peptide agents have recently got much consideration due to their capacity to prevail over bacterial resistance and have come into sight as a newer prospective category of antibacterial agents with new modes of actions.²⁶⁻²⁸ Here, a hexapeptide template was chosen from bovine lactoferricin protein as a Trp and Arg rich amino acid sequence with reported known antimicrobial efficacy which was obtained through the screening of the hexapeptide combinatorial library.²⁹ The designed sequence of Hexapeptide analogue included Arg-Arg-Trp-Trp-Arg-Phe-Gly-Gly-Cys where N-terminal was acylated and at C-terminal was amidated.

5.1 *In-silico* studies

The various factors influence the antibacterial activity of cationic peptides which include:

- Net positive charge for increased interaction with anionic lipid layer of bacterial cell-wall
- Hydrophobicity for insertion into the membrane
- Flexibility of the peptide to transition to membrane interacting conformation

The designed sequence of peptide was analysed and these properties calculated by the predictive tool available at Antimicrobial Peptide Database v2.34 (APD2) using the Antimicrobial Peptide Database (APD) and the results showed that the total hydrophobic ratio was found to be 44%, and net charge was +3 and the number of rotatable bonds which is a simple measure of conformational flexibility was found to be 41. The hydrophobicity of the peptide governs the extent to which the peptide can effectively permeate into the lipid bilayer. Besides this, the net positive charge of + 3 which is due to the basic residue (Arg or Lys) also augments in its antimicrobial action. The presence of Arg and Trp rich residues are known to play a vital role in insertion into the cell-membrane. It is reported and well-established by solid state NMR results that the electrostatic interactions of guanidinium side chain of Arg with phosphate groups form ' guanidinium-phosphate salt bridges' to stabilize the protein-membrane interaction.³⁰⁻³² Further the Trp residues provide favorable cation- π interaction for stacking and stabilisation in aqueous solutions.^{33,34}

For the docking studies, PDB ID selected is 3VMA, the crystal structure of *E. coli* PBP1b a bifunctional peptidoglycan glycosyltransferase which represents a structural platform of transglycosylase, especially for Gram-negative bacteria for the antibacterial drug designing. Molecular docking was performed to understand the interaction between the receptor (bacterial glycosyltransferase protein) and ligand (hexapeptide analogue-AMP) molecule (Fig. 1). Docking results revealed the binding affinity in terms of glide GScore of -9.22. The contribution of this docking score was due to H-bond, electrostatic and hydrophobic interactions where the electrostatic and hydrophobic interactions were much higher than the co-crystallized molecule moenomycin ($C_{69}H_{106}N_5O_{34}P$).

The crucial 3VMA-Mol-1 interactions could be defined by ligands interacting through both hydrogen and electrostatic bonding to Asn-143, Arg-364, Ser-358, Glu-323, Lys-274, Glu-281, Thr-257 and with Glu-233 and their contributions were significant for ligand

binding. These critical anchoring residues were also found to be constant with further studies. The comprehensive study was done to determine the hydrophobic and hydrophilic domains needed for high anti-bacterial activity and low hemolytic activity. The reference molecule was showing different interactions except Glu-281, which was also confirmed by the contribution of GScore. It showed higher hydrogen bonding rather than electrostatic and hydrophobic interaction. This may be due to the different mode of action possibilities.

It is reported that only peptides with an optimal binding affinity toward the outer membrane could penetrate into the inner layer of a bacterial cell.³⁵ Categorically electrostatic or polar interaction were found in two mode one as negative charge created at amino acid residue of target protein like Glu-233, Glu-281 and Glu-323 while in other negative charge was created on ligand side like on Arg-364, Lys-274 and Ser-358. The hydrophobic periphery was created by Ala-254, Ala-258, Ala-265, Tyr-310, Val-314, Tyr-315, Val-354 and Ala-357. The negatively charged bacterial membranes and the cationic charge of the peptide offer an ideal interaction to attract the peptides to these cells, and the electrostatic forces are important for the selectivity and their interactions.^{36,30,33}

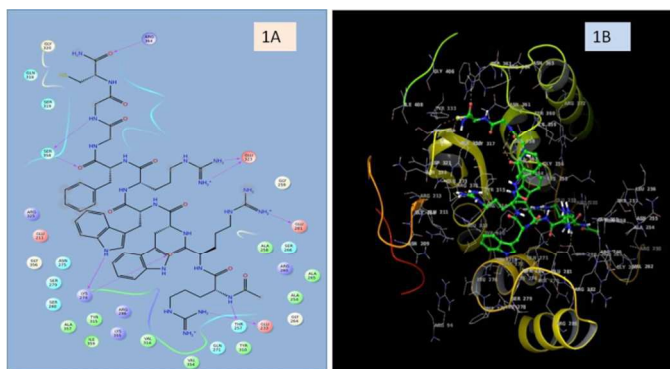


Fig. 1 Ligand-target protein interaction depicting the possible non-covalent (especially hydrogen bonds) binding of important anchoring residues present in the active site of bacterial protein to the hexapeptide in (1A) Two-dimensional pictorial representation mode and (1B) in Three dimensional mode view of active site of target protein (PBDID: 3VMA) with the designed peptide.

5.2 Peptide Synthesis

The newly designed hexapeptide analogue (AMP) was such designed such that the template RRWWRF was the targeting moiety while the tripeptide (GGC) chain was chosen as a chelating moiety for radiotracer (^{99m}Tc) conjugation. The proposed structure of ^{99m}Tc-nonapeptide (^{99m}Tc-AMP) shows that a strong chelation with radiotracer ^{99m}Tc by N4 configuration that is well-established chelation strategy.³⁷ Peptide Retention-time by HPLC was found to be 11.96 min. The mass spectrum of HPLC purified AMP is depicted in Fig. 2 that confirmed the synthesis of the final product as the expected molecular weight of the synthesized peptide sequence was 1264.5 and the observed mass was found to be Mass; m/z =

1288.6 -found [M+ Na]⁺ (Fig. 2).

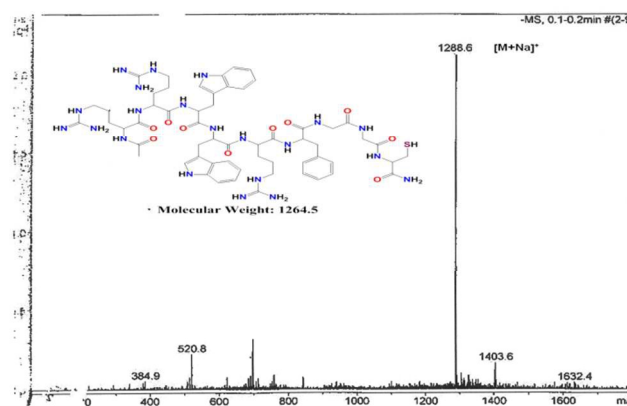


Fig. 2 The mass spectrum of synthesized AMP peptide

5.3 In-Vitro Studies

5.3.1 Antimicrobial activity assessment studies

The antimicrobial activity of the hexapeptide analogue was assessed against the six bacterial strains namely *Salmonella enteritidis*, *Escherichia coli* (*E. Coli*), *Listeria innocua*, *Micrococcus luteus* and *Staphylococcus aureus* and the MIC values against these strains are shown in Table 1. The hexapeptide analogue (AMP) demonstrated a strong inhibitory activity against the Gram-negative bacteria *E. coli* with the minimum inhibitory concentration (MIC) value of 12.1 μ M. This data correlates with the docking study findings that the designed hexapeptide has the excellent inhibitory action against the *E. coli* strain.

Micro-organism	Mean Minimum Inhibition conc. values for the synthesized peptide (AMP) (μ M)
<i>Salmonella enteritidis</i>	35
<i>Escherichia coli</i>	12.1
<i>Listeria innocua</i>	17.1
<i>Micrococcus luteus</i>	30.4
<i>Staphylococcus aureus</i>	21.0

The minimum inhibitory concentration (MIC) of the peptide was determined in a microtiter plate assay system after 24 h incubation at 37 °C.

Table 1 In vitro anti-bacterial activity was determined against the different bacterial strains. Data expressed as mean Minimum Inhibitory Concentration (MIC) values in units of μ M.

5.3.2 Hemolytic Activity Studies

Hemolytic activity is utilized to measure the in-vivo toxicity of the synthesized peptide. The short peptide synthesised in this study was essentially non-hemolytic (< 5%) as illustrated in Fig. 3. It is reported that there exists a strong relationship between the number of aromatic acids such as tryptophan present in the sequence of the antimicrobial peptide and its hemolytic action where peptide-sequence with only three or fewer tryptophan residues are predominately antimicrobial and non-toxic.³⁸

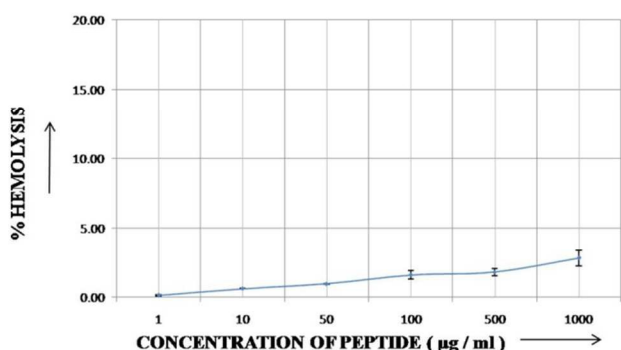


Fig. 3 Hemolytic activity of Hexapeptide analogue (AMP) on human erythrocytes. The dose-dependent haemolytic effects were carried out from 10^0 to 10^3 $\mu\text{g/ml}$ of the synthesised peptide. The 100% hemolysis of erythrocytes was carried out by addition of Triton-X 100. Error bars represent SD.

5.3.3 Radio labeling studies

The radiolabeling of the newly synthesized AMP was carried out by the method previously described³⁹ and the radiochemical purity was assessed by chromatographically was found to be more than 98%. The structural similarity of the N4 configuration and the analogous chromatographic nature, it seems rational to assume that the $^{99\text{m}}\text{Tc}$ -complex of hexapeptide analogue will have a similar structure as for $^{99\text{m}}\text{Tc}$ -MAG3 derivatives, as the complex in which the nitrogen atoms of amide groups are deprotonated and a bond is formed with the technetium oxo-core, which, additionally is bound to the nitrogen atom of amine group. Even up to 6 h, the percentage labeling efficiency of $^{99\text{m}}\text{Tc}$ labeled AMP was found to be 94.5%, implying that the radiotagging with the peptide was quite stable and fit for *in-vivo* evaluation studies.

5.4 In- Vivo Studies

5.4.1 Blood- Kinetics Studies

The pharmacokinetic profile of radiolabeled peptides demonstrated biexponential clearance pattern with $T_{1/2\alpha}$ and $T_{1/2\beta}$ calculated were found to be 6.7 min and 79.2 min respectively (Table 2) The short sequence of peptides are known for their rapid clearance from the systemic circulation, and this feature is confirmed by $25.84\% \pm 1.72$ of the blood associated radioactivity at 5 min post injection which could be further utilized for non-invasive diagnostic imaging studies with the aim of early detection of the infectious site.

HALF-LIFE	UNIT	VALUE
$T_{1/2\alpha}$	Min	6.7
$T_{1/2\beta}$	Min	79.2

Table 2 The pharmacokinetic data of $^{99\text{m}}\text{Tc}$ - labeled AMP (n = 3)

5.4.2 Tissue distribution Studies

The specific organ distribution of radiolabeled peptide after *i. v.* administration was expressed as percentage injected dose per gram of organ (% ID per gm) in mice and is depicted in Fig. 4. Since the fast clearance from the blood circulation was established in the blood-kinetics data, the samples of urine and faeces at each time-interval were also collected along with the organs. The concentration of radiolabeled peptide was found to be maximum in organs like Kidneys (33 ± 5.12) followed by Liver (10.77 ± 1.23) and Spleen (3.1 ± 0.31) at 1 h post injection. The radiolabel also demonstrated negligible uptake in the non-target region like abdominal region with low blood-pool activity. This attribute facilitates a faster specific uptake in the target site which is a desirable characteristic for a good infection imaging agent.

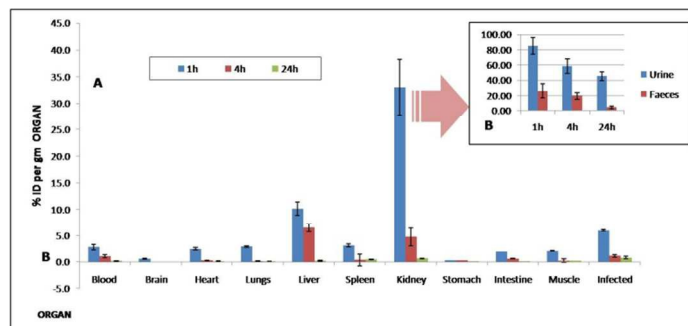


Fig. 4 Organ-distribution in infection model of BALB/c mice at 1 h, 4 h and 24 h after intravenous administration (*i.v.*) of $100\mu\text{l}$ of $^{99\text{m}}\text{Tc}$ labeled AMP (40KBq). The data (in inset) represents percent injected dose per gm of the excreta: urine and faeces samples. Data expressed as percent injected dose per gm organ/tissue \pm S.D. of 3 animals.

5.3.3 Gamma Scintigraphic Studies

The gamma scintigraphic study was designed to carry out three sets of experiments in normal rats and in *E. coli* infected animal models. Firstly, the whole body imaging carried out in normal rat confirmed the fast renal clearance at 1 h and 4 h post administration as shown in Fig. 5A and Fig. 5B respectively. The animal models of infection and inflammation were developed in BALB/c mice and Fig. 6A and Fig. 6B are infected mice scanned at 1h and 4h respectively while Fig. 6C and Fig. 6D represent the inflammation model imaged at 1h and 4h respectively. The higher uptake of the radioactivity was observed in the infected muscle in comparison to the contra-lateral area was observed at 1 h post injection for the group A as shown in Fig. 6B while for both contralateral and inflamed side, similar uptake was observed for the group B in case of Fig. 6C and Fig. 6D.

For the blocking experiments in scintigraphy, the animals used were *E. coli* infected rats. To one group L, the radiolabeled peptide alone was administered while to the group R, the pre-blocking with the cold unlabeled peptide was carried out prior the administration of the radiolabeled peptide. Since, the peptides are fast cleared from the systemic circulation; the scintigraphic scan was scheduled at 1 h post injection. The Fig. 7A and Fig. 7B represent the imaging done at 1 h and 4 h post administration and Fig. 7C represent zoomed scan of

the lower region of the rats imaged at 4 h. The higher uptake in the group L as depicted in Fig. 7C proved the specific targeting of the given peptide to the infectious lesion.

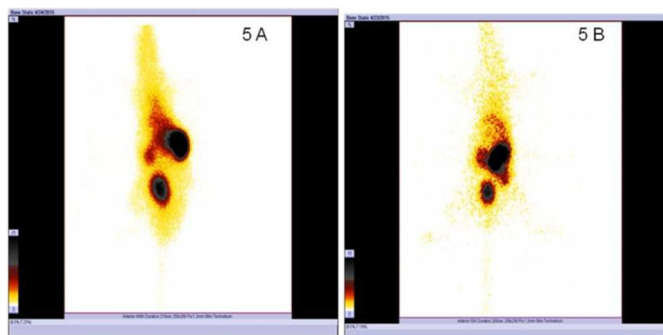


Fig. 5 Whole-body scintigraphic scan carried out in normal rat at 5A) 1 h 5B) 4 h post i.v. administration of ^{99m}Tc labeled AMP.

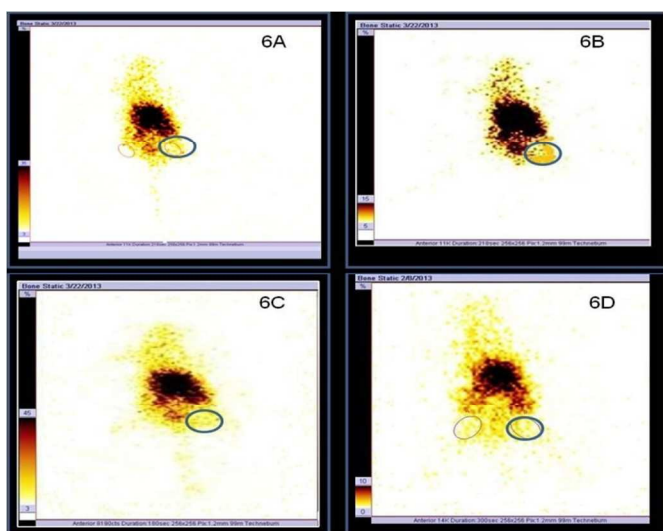


Fig. 6 Scintigraphic studies carried out after intravenous administration (i.v.) of ^{99m}Tc labeled AMP in BALB/c mice models where 6A) and 6B) represent infection model imaged at 1 h and 4 h respectively. The images 6C) and 6D), here stand for inflammation model scanned at 1 h and 4 h respectively. The black oval shape points at the site of infection/ inflammation.

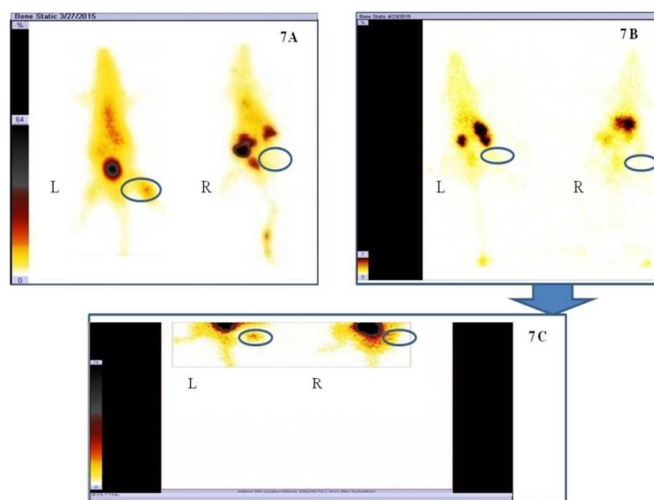


Fig. 7 Gamma scintigraphic scans carried out in infection induced rats. The Rat -L represent the animals which were administered the radiolabeled AMP alone and the Rat-R stand for the animals which were administered cold unlabeled AMP prior the injection of ^{99m}Tc labeled AMP. 7A) and 7B) are gamma Images taken 1 h and 4 h p.i. respectively. 7C) is zoomed up scan taken at 4h p.i. to pinpoint the lesion.

Note: The black oval shape marks the site of infection

3.54 Histopathological Studies

The microscopical appearances of the Sections from muscle sample are depicted in Fig. 8B which showed several bacterial aggregates of *E. coli* with a pronounced acute inflammatory cell infiltration around the bacteria as seen by the presence of numerous polymorph nuclear neutrophilic cells. The control group animal showed only normal skeletal muscle as shown in Fig. 8A.

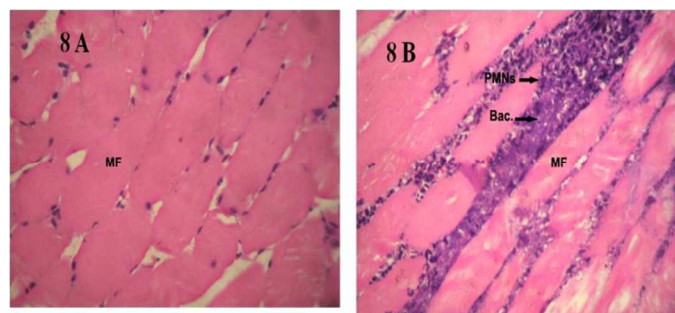


Fig. 8 Histopathological data is represented by A) Control Sample section showed normal skeletal muscle fibres and B) Infected Sample Section shows presence of numerous Bacterial groups along with Polymorphonuclear Cell Infiltration around the bacteria.

Note: MF = Muscle fibre, Bac. = Bacteria, PMNs = Polymorphonuclear Neutrophilic Cells.)

6. Conclusion

In search for developing a novel peptide-based infection imaging agent, we have rationally designed a new nonapeptide from the known sequence of the antimicrobial peptide. *In vitro* antimicrobial study suggested best efficacy against the *E. coli* strains and *in-silico* studies corroborated these findings. Since the agent exhibited fast kinetics, the infectious lesion induced in a murine model was detected by *in-vivo* gamma scintigraphy after administration of radiolabeled hexapeptide analogue as early as 1h post injection. These results gave a simple, insightful initiative into pharmacokinetics and preclinical considerations of ^{99m}Tc conjugate with the designed peptide. Further experiments are being planned to take this imaging agent to clinical evaluation after validating in other animal models of *E. coli* infections.

Acknowledgements

We thank Dr R. P. Tripathi, Director INMAS, for providing necessary facilities and infrastructure. The work was supported by Defence Research and Development Organization, Ministry of Defence, under R&D project INM-311.

Notes and references

Division of Cyclotron and Radiopharmaceutical Sciences, Institute of Nuclear Medicine and Allied Sciences, Brig. S. K. Mazumdar Road, Delhi-110054, India.

References

- A. J. Huh and Y. J. Kwon, *Journal of controlled release : official journal of the Controlled Release Society*, 2011, **156**, 128-145.
- M. R. Yeaman and N. Y. Yount, *Pharmacological reviews*, 2003, **55**, 27-55.
- M. Castanho and N. Santos, *Peptide drug discovery and development: translational research in academia and industry*, John Wiley & Sons, 2011.
- G. Wang, *Antimicrobial peptides: discovery, design and novel therapeutic strategies*, CABI, 2010.
- Y. Li, Q. Xiang, Q. Zhang, Y. Huang and Z. Su, *Peptides*, 2012, **37**, 207-215.
- A. Giuliani, G. Pirri, A. Bozzi, A. Di Giulio, M. Aschi and A. Rinaldi, *Cellular and Molecular Life Sciences*, 2008, **65**, 2450-2460.
- R. E. Hancock and D. S. Chapple, *Antimicrobial agents and chemotherapy*, 1999, **43**, 1317-1323.
- K. A. Brogden, *Nature Reviews Microbiology*, 2005, **3**, 238-250.
- H. Jenssen, P. Hamill and R. E. Hancock, *Clinical microbiology reviews*, 2006, **19**, 491-511.
- S. E. Blondelle and R. A. Houghten, *Trends in biotechnology*, 1996, **14**, 60-65.
- E. J. Martin and R. E. Critchlow, *Journal of combinatorial chemistry*, 1999, **1**, 32-45.
- G. R. Marshall, *Tetrahedron*, 1993, **49**, 3547-3558.
- G. Wang, X. Li and Z. Wang, *Nucleic acids research*, 2009, **37**, D933-D937.
- J. Choi and E. Moon, *J. Microbiol. Biotechnol*, 2009, **19**, 792-802.
- H. J. Vogel, D. J. Schibli, W. Jing, E. M. Lohmeier-Vogel, R. F. Eband and R. M. Eband, *Biochemistry and Cell Biology*, 2002, **80**, 49-63.
- A. Kaul, P. P. Hazari, H. Rawat, B. Singh, T. C. Kalawat, S. Sharma, A. K. Babbar and A. K. Mishra, *International Journal of Infectious Diseases*, 2013, **17**, e263-e270.
- G. Lucignani, *European journal of nuclear medicine and molecular imaging*, 2007, **34**, 1873-1877.
- A. Lupetti, M. M. Welling, E. K. Pauwels and P. H. Nibbering, *The Lancet infectious diseases*, 2003, **3**, 223-229.
- M. Liberatore, A. Pala, S. Scaccianoce, C. Anagnostou, U. Di Tondo, E. Calandri, P. D'Elia, M. D. Gross and D. Rubello, *Journal of Nuclear Medicine*, 2009, **50**, 823-826.
- G. Ferro-Flores, C. A. de Murphy, M. Pedraza-López, L. Meléndez-Alafort, Y.-M. Zhang, M. Rusckowski and D. J. Hnatowich, *Nuclear medicine and biology*, 2003, **30**, 597-603.
- G. Version, LLC, New York, NY, 2005.
- R. A. Friesner, J. L. Banks, R. B. Murphy, T. A. Halgren, J. J. Klicic, D. T. Mainz, M. P. Repasky, E. H. Knoll, M. Shelley and J. K. Perry, *Journal of medicinal chemistry*, 2004, **47**, 1739-1749.
- R. A. Houghten, *Proceedings of the National Academy of Sciences*, 1985, **82**, 5131-5135.
- G. Diamond, D. Laube and M. Klein-Patel, *Journal*, 2004.
- K. Reddy, R. Yedery and C. Aranha, *International journal of antimicrobial agents*, 2004, **24**, 536-547.
- D. Andreu and L. Rivas, *Biopolymers*, 1998, **47**, 415-433.
- Y. Chen, C. T. Mant, S. W. Farmer, R. E. Hancock, M. L. Vasil and R. S. Hodges, *Journal of Biological Chemistry*, 2005, **280**, 12316-12329.
- W. Jing, H. Hunter, J. Hagel and H. Vogel, *The Journal of peptide research*, 2003, **61**, 219-229.
- M. B. Strøm, Ø. Rekdal and J. S. Svendsen, *Journal of Peptide Science*, 2002, **8**, 431-437.
- M. Hong and Y. Su, *Protein Science*, 2011, **20**, 641-655.
- Y. Su, S. Li and M. Hong, *Amino acids*, 2013, **44**, 821-833.
- M. R. Lourenzoni, A. M. Namba, L. Caseli, L. Degreve and M. E. Zaniquelli, *The journal of physical chemistry. B*, 2007, **111**, 11318-11329.
- W. M. Yau, W. C. Wimley, K. Gawrisch and S. H. White, *Biochemistry*, 1998, **37**, 14713-14718.
- D. I. Chan, E. J. Prenner and H. J. Vogel, *Biochimica et biophysica acta*, 2006, **1758**, 1184-1202.
- L. H. Kondejewski, M. Jelokhani-Niaraki, S. W. Farmer, B. Lix, C. M. Kay, B. D. Sykes, R. E. W. Hancock and R. S. Hodges, *Journal of Biological Chemistry*, 1999, **274**, 13181-13192.
- D. J. Schibli, R. F. Eband, H. J. Vogel and R. M. Eband, *Biochemistry and cell biology*, 2002, **80**, 667-677.
- H. P. Vanbilloen, G. M. Bormans, M. J. De Roo and A. M. Verbruggen, *Nuclear medicine and biology*, 1995, **22**, 325-338.
- L. T. Nguyen, J. K. Chau, N. A. Perry, L. De Boer, S. Zaat and H. J. Vogel, *PLoS one*, 2010, **5**, e12684.
- M. L. Thakur, V. R. Pallela, P. M. Consigny and P. S. Rao, *The Journal of Nuclear Medicine*, 2000, **41**, 161.